Recent studies on ~~the dipole~~ nuclear excitations within the Subtracted Second RPA

Danilo Gambacurta
gambacurta@lns.infn.it
INFN-LNS Catania

Giant and Soft Modes of Excitation in Nuclear Structure and Astrophysics
Trento, October 24-28, 2022

Outline

- Theoretical models: RPA and Second RPA (SRPA)
- Improving on the SRPA: the Subtracted SRPA (SSRPA)
- Dipole excitations: Pygmy states and GDR
- Beyond-mean-field effects on the symmetry energy and its slope
- Low-lying monopole excitations: soft modes
- Gamow-Teller excitations and Beta-decay
- Conclusions

The Random Phase Approximation (RPA)

- The RPA is a widely used approximation for the description of NEs
- Very successful especially within the Energy Density Functional framework (interactions á la Skyrme or Gogny, covariant versions)
- It provides global properties: centroid energies and total strength

However, extensions of the RPA are required for:

- Spreading Width
- Fine Structure and Strength Fragmentation
- Low Lying excitations in closed shell nuclei
- Double exctiations and Anharmonicities, ...

The Second RPA (SRPA): more general excitation operators are introduced

The Method of the Equations of Motion

Set of exact eigenstates of the Hamiltonian H

$$H|\nu\rangle = E_\nu \mid \nu\rangle$$

where $\mid 0\rangle$ is the ground state with energy E_0.

Phonon Operators

Let us introduce the operators $Q's$:

$$Q_\nu^\dagger \mid 0\rangle = \mid \nu\rangle, \qquad Q_\nu \mid 0\rangle = 0.$$

Equations of Motion:

$$\langle 0 \mid \left[\delta Q, [H, Q_\nu^\dagger]\right] \mid 0\rangle = \omega_\nu \langle 0 \mid [\delta Q, Q_\nu^\dagger] \mid 0\rangle$$

where

$$\omega_\nu = E_\nu - E_0.$$

Phonon Operators: RPA vs SRPA

Random Phase Approximation (RPA)

$$Q_\nu^\dagger = \underbrace{\sum_{ph} X_{ph}^{(\nu)} \underbrace{a_p^\dagger a_h}_{\text{1p-1h}} - \sum_{ph} Y_{ph}^{(\nu)} \underbrace{a_h^\dagger a_p}_{\text{1h-1p}}}_{\text{Only Landau Damping, Centroid Energy and Total Strength of GRs}}$$

Second Random Phase Approximation (SRPA)

$$Q_\nu^\dagger = \sum_{ph}(X_{ph}^{(\nu)} a_p^\dagger a_h - Y_{ph}^{(\nu)} a_h^\dagger a_p)$$

$$+ \underbrace{\sum_{p_1<p_2,h_1<h_2} (X_{p_1 h_1 p_2 h_2}^{(\nu)} \underbrace{a_{p_1}^\dagger a_{h_1} a_{p_2}^\dagger a_{h_2}}_{\text{2p-2h}} - Y_{p_1 h_1 p_2 h_2}^{(\nu)} \underbrace{a_{h_1}^\dagger a_{p_1} a_{h_2}^\dagger a_{p_2}}_{\text{2h-2p}})}_{\textbf{Spreading Width, Fragmentation}\text{, Double GRs and Anharmonicites, Low-Lying States}}$$

RPA Excitation Operators and Equations

RPA Phonon Operators

$$Q_\nu^\dagger = \sum_{ph} X_{ph}^{(\nu)} a_p^\dagger a_h - \sum_{ph} Y_{ph}^{(\nu)} a_h^\dagger a_p$$

RPA Equations of Motion (1$\mapsto$ 1p1h)

$$\begin{pmatrix} \mathcal{A}_{11} & \mathcal{B}_{11} \\ -\mathcal{B}_{11}^* & -\mathcal{A}_{11}^* \end{pmatrix} \begin{pmatrix} \mathcal{X}_1^\nu \\ \mathcal{Y}_1^\nu \end{pmatrix} = \omega_\nu \begin{pmatrix} \mathcal{X}_1^\nu \\ \mathcal{Y}_1^\nu \end{pmatrix}$$

SRPA Phonon Operators

$$Q_\nu^\dagger = \sum_{ph} (X_{ph}^{(\nu)} a_p^\dagger a_h - Y_{ph}^{(\nu)} a_h^\dagger a_p)$$

$$+ \sum_{p_1<p_2, h_1<h_2} (X_{p_1 h_1 p_2 h_2}^{(\nu)} a_{p_1}^\dagger a_{h_1} a_{p_2}^\dagger a_{h_2} - Y_{p_1 h_1 p_2 h_2}^{(\nu)} a_{h_1}^\dagger a_{p_1} a_{h_2}^\dagger a_{p_2})$$

SRPA Equations of Motion (1$\mapsto$ 1p1h, 2$\mapsto$ 2p2h)

$$\begin{pmatrix} \mathcal{A}_{11} & \mathcal{A}_{12} & \mathcal{B}_{11} & \mathcal{B}_{12} \\ \mathcal{A}_{21} & \mathcal{A}_{22} & \mathcal{B}_{21} & \mathcal{B}_{22} \\ -\mathcal{B}_{11}^* & -\mathcal{B}_{12}^* & -\mathcal{A}_{11}^* & -\mathcal{A}_{12}^* \\ -\mathcal{B}_{21}^* & -\mathcal{B}_{22}^* & -\mathcal{A}_{21}^* & -\mathcal{A}_{22}^* \end{pmatrix} \begin{pmatrix} \mathcal{X}_1^\nu \\ \mathcal{X}_2^\nu \\ \mathcal{Y}_1^\nu \\ \mathcal{Y}_2^\nu \end{pmatrix} = \omega_\nu \begin{pmatrix} \mathcal{X}_1^\nu \\ \mathcal{X}_2^\nu \\ \mathcal{Y}_1^\nu \\ \mathcal{Y}_2^\nu \end{pmatrix}$$

SRPA Excitation Operators and Equations

SRPA Phonon Operators

$$Q_\nu^\dagger = \sum_{ph} (X_{ph}^{(\nu)} a_p^\dagger a_h - Y_{ph}^{(\nu)} a_h^\dagger a_p)$$

$$+ \sum_{p_1<p_2,h_1<h_2} (X_{p_1 h_1 p_2 h_2}^{(\nu)} a_{p_1}^\dagger a_{h_1} a_{p_2}^\dagger a_{h_2} - Y_{p_1 h_1 p_2 h_2}^{(\nu)} a_{h_1}^\dagger a_{p_1} a_{h_2}^\dagger a_{p_2})$$

SRPA Equations of Motion (1$\mapsto$ 1p1h, 2$\mapsto$ 2p2h)

$$\begin{pmatrix} \mathcal{A}_{11} & \mathcal{A}_{12} & \mathcal{B}_{11} & \mathcal{B}_{12} \\ \mathcal{A}_{21} & \mathcal{A}_{22} & \mathcal{B}_{21} & \mathcal{B}_{22} \\ -\mathcal{B}_{11}^* & -\mathcal{B}_{12}^* & -\mathcal{A}_{11}^* & -\mathcal{A}_{12}^* \\ -\mathcal{B}_{21}^* & -\mathcal{B}_{22}^* & -\mathcal{A}_{21}^* & -\mathcal{A}_{22}^* \end{pmatrix} \begin{pmatrix} \mathcal{X}_1^\nu \\ \mathcal{X}_2^\nu \\ \mathcal{Y}_1^\nu \\ \mathcal{Y}_2^\nu \end{pmatrix} = \omega_\nu \begin{pmatrix} \mathcal{X}_1^\nu \\ \mathcal{X}_2^\nu \\ \mathcal{Y}_1^\nu \\ \mathcal{Y}_2^\nu \end{pmatrix}$$

Computationally very demanding

- Only recently full large scale SRPA calculations have been performed [a]
- Model spaces large enough to preserve EWSRs
- No approximation in the evaluation of the matrix elements

[a] P. Papakonstantinou and R. Roth, PLB 671, 356 (2009); D.G et al. PRC 81, 054312 (2010)

.

RPA Matrices (1p1h configurations)

$$A_{1,1'} = \langle HF \mid \left[a_h^\dagger a_p, [H, a_{p'}^\dagger a_{h'}]\right] \mid HF\rangle$$

$$B_{1,1'} = -\langle HF \mid \left[a_h^\dagger a_p, [H, a_{h'}^\dagger a_{p'}]\right] \mid HF\rangle.$$

SRPA Matrices (1p1h and 2p2h configurations)

$$A_{1,2} = A_{2,1}^* = \left\langle HF \middle| \left[a_h^\dagger a_p, [H, a_{p_1}^\dagger a_{p_2}^\dagger a_{h_1} a_{h_2}]\right] \middle| HF \right\rangle$$

$$A_{2',2} = \left\langle HF \middle| \left[a_{h_2'}^\dagger a_{h_1'}^\dagger a_{p_2'} a_{p_1'}, [H, a_{p_1}^\dagger a_{p_2}^\dagger a_{h_1} a_{h_2}]\right] \middle| HF \right\rangle$$

$$B_{1,2} = B_{2,1}^* = -\left\langle HF \middle| \left[a_p^\dagger a_h, [H, a_{p_1}^\dagger a_{p_2}^\dagger a_{h_1} a_{h_2}]\right] \middle| HF \right\rangle = 0$$

$$B_{2',2} = -\left\langle HF \middle| \left[a_{p_1'}^\dagger a_{p_2'}^\dagger a_{h_1'} a_{h_2'}, [H, a_{p_1}^\dagger a_{p_2}^\dagger a_{h_1} a_{h_2}]\right] \middle| HF \right\rangle = 0$$

Quasi Boson Approximation (QBA) **is still used**

The vacuum of the Q's operators $\mid 0\rangle$ is not known:

$$\mid 0\rangle \mapsto \mid HF\rangle, \qquad \left[a_p^\dagger a_h, a_{h'}^\dagger a_{p'}\right] \approx \delta_{pp'}\delta_{hh'}$$

The Subtraction procedure

Large scale SRPA calculations have shown that:

- The SRPA strength distribution is sistematically shifted towards lower energies compared to the RPA one
- This shift is very strong ($\simeq$ 3-4 MeV), RPA description often spoiled

Origins and Causes:

1. Quasi Boson Approximation and stability problems in SRPA
2. Use of effective interactions in beyond-mean field methods

The Subtraction procedure (I. Tselyaev Phys. Rev. C 75, 024306 (2007))

- Designed for beyond RPA approaches
- It restores the Thouless theorem, e.g. instabilities are removed
- Static ($\omega = 0$) limit of the SRPA imposed to be equal to the RPA one

From SRPA to an Energy dependent RPA-like problem

- The SRPA problem as an energy-dependent RPA problem

$$A_{1,1'} \mapsto \tilde{A}_{1,1'}(\omega) = A^{RPA}_{1,1'} + \sum_{2,2'} A_{1,2}(\omega + i\eta - A_{2,2'})^{-1} A_{2',1'} = A^{RPA}_{1,1'} + A^{Cor}_{1,1'}(\omega)$$

From SRPA to an Energy dependent RPA-like problem

- The SRPA problem as an energy-dependent RPA problem

$$A_{1,1'} \mapsto \tilde{A}_{1,1'}(\omega) = A^{RPA}_{1,1'} + \sum_{2,2'} A_{1,2}(\omega + i\eta - A_{2,2'})^{-1} A_{2',1'} = A^{RPA}_{1,1'} + A^{Cor}_{1,1'}(\omega)$$

The Subtraction procedure is SRPA (SSRPA)

- Subtraction of the zero–frequency limit of the SRPA correction

$$A^{Cor}_{1,1'} \mapsto \tilde{A}^{Cor}_{1,1'}(\omega) = A_{1,1'}(\omega) - A_{1,1'}(\omega = 0) \Rightarrow$$

$$\tilde{A}_{1,1'}(\omega = 0) = A^{RPA}_{1,1'}$$

$$\Rightarrow \Pi^{SSRPA}(\omega = 0) = \Pi^{RPA}$$

From SRPA to an Energy dependent RPA-like problem

- The SRPA problem as an energy-dependent RPA problem

$$A_{1,1'} \mapsto \tilde{A}_{1,1'}(\omega) = A^{RPA}_{1,1'} + \sum_{2,2'} A_{1,2}(\omega + i\eta - A_{2,2'})^{-1} A_{2',1'} = A^{RPA}_{1,1'} + A^{Cor}_{1,1'}(\omega)$$

The Subtraction procedure is SRPA (SSRPA)

- Subtraction of the zero–frequency limit of the SRPA correction

$$A^{Cor}_{1,1'} \mapsto \tilde{A}^{Cor}_{1,1'}(\omega) = A_{1,1'}(\omega) - A_{1,1'}(\omega = 0) \Rightarrow$$

$$\tilde{A}_{1,1'}(\omega = 0) = A^{RPA}_{1,1'}$$

$$\Rightarrow \Pi^{SSRPA}(\omega = 0) = \Pi^{RPA}$$

Numerical implementation

- Subtraction performed in diagonal approximation, e.g. $A_{2,2'} \approx \delta_{2,2'} A_{2,2}$
- Full subtraction recently performed (GT strength) [a]

[a] DG, M. Grasso, J. Engel, Physical Review Letters 125, 212501 (2020)

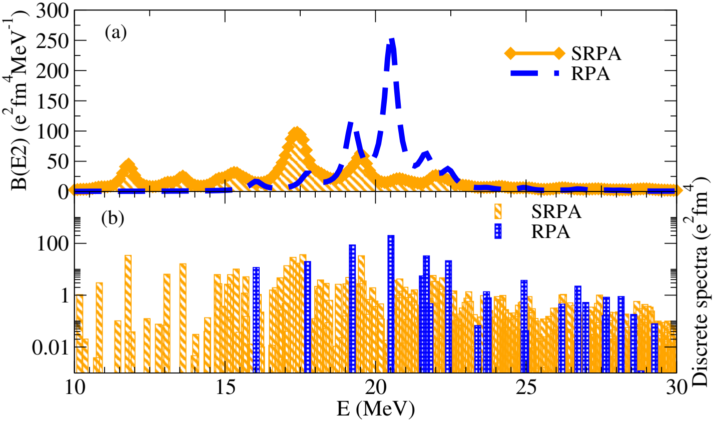

D. G., M. Grasso and J.Engel, Phys. Rev. C 92 , 034303 (2015)

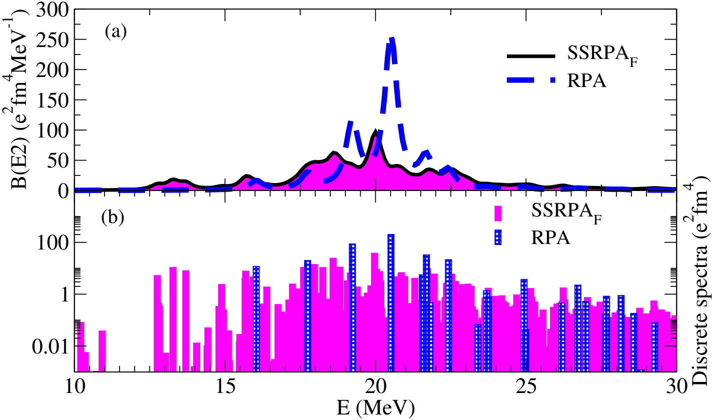

D. G., M. Grasso and J.Engel, Phys. Rev. C 92 , 034303 (2015)

Low-lying dipole response in ^{48}Ca: Motivation

- Experimental low-lying dipole (from 5 to 10 MeV) response in ^{48}Ca stronger than in ^{40}Ca
- Pygmy Dipole Resonance (PDR) type?
- Not described in relativistic and non-relativistic RPA models
- What happens in SRPA [a] ?
- and in the SSRPA [b] ?

[a] D. G. , M. Grasso, and F. Catara, Phys. Rev. C 84, 034301 (2011)
[b] D. G., M. Grasso and O. Vasseur, Physics Letters B 777 (2018) 163–168

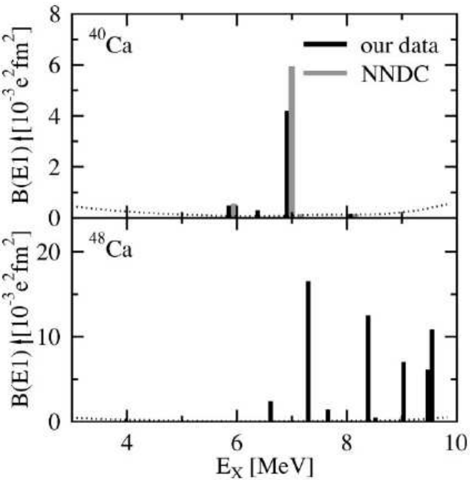

$\sum$ B(E1)=5.1 $\pm$ 0.8 (10^{-3}e^{2}fm^2),

$\sum$ B(E1)=68.7 $\pm$ 7.5 (10^{-3}e^{2}fm^2),

From T. Hartmann *et al.*, PRC 65, 034301, (2002)

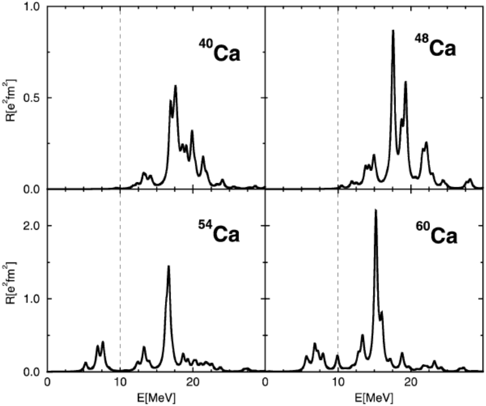

Fig. 5. RRPA isovector dipole strength distributions in Ca isotopes. The thin dashed line tentatively separates the region of giant resonances from the low-energy region below 10 MeV.

From D. Vretenar *et al.*, Nucl. Phys. A 692, 496 (2001)

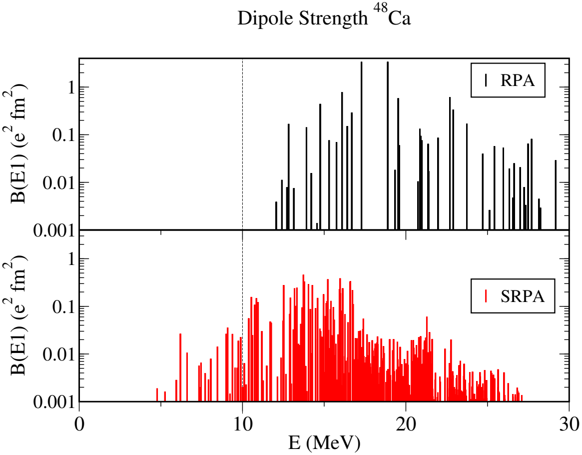
Dipole Strength ^{48}Ca
RPA
SRPA
B(E1) (e^2 fm^2)
B(E1) (e^2 fm^2)
1
0.1
0.01
0.001
0
10
20
30
E (MeV)

RPA and SRPA Dipole Strength

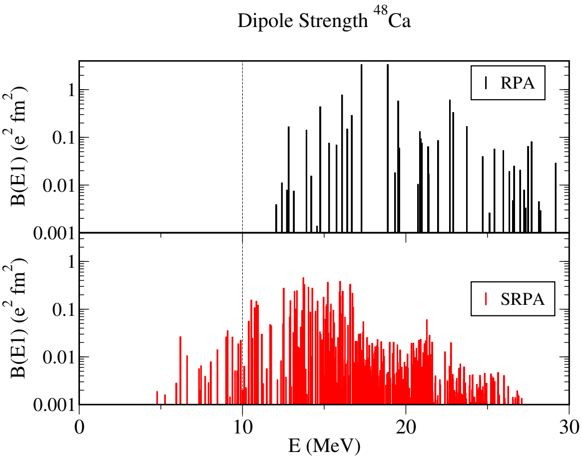

SRPA provides the strength below 10 MeV, but total strength is overestimated.

1p1h and 2p2h contents

$$\langle \nu|\nu\rangle = \sum_{ph} (|\ X^{\nu}_{ph}\ |^2 - |\ Y^{\nu}_{ph}\ |^2) + \sum_{p_1<p_2,h_1<h_2} (|\ X^{\nu}_{p_1h_1p_2h_2}\ |^2 - |\ Y^{\nu}_{p_1h_1p_2h_2}\ |^2)$$

$$= \qquad N_1 \qquad + \qquad N_2 \qquad = 1$$

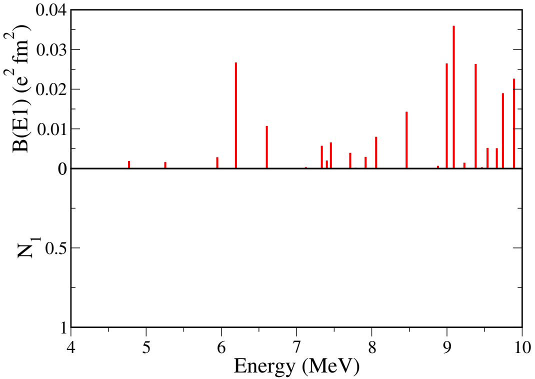

$1p1h$-$2p2h$ composition of the states

$1p1h$ and $2p2h$ contents

$$\langle \nu|\nu\rangle = \sum_{ph}(|\, X^{\nu}_{ph}\,|^2 - |\, Y^{\nu}_{ph}\,|^2) + \sum_{p_1<p_2, h_1<h_2}(|\, X^{\nu}_{p_1h_1p_2h_2}\,|^2 - |\, Y^{\nu}_{p_1h_1p_2h_2}\,|^2)$$

$$= \quad N_1 \quad + \quad N_2 \quad = 1$$

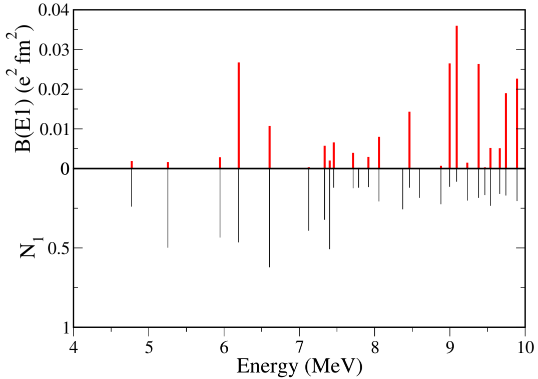

ph conf.	E = 6.19 MeV			F^{λ}_{ph}
	E (MeV)	A_{ph}	$b_{ph}(E1)$	
$(1f_{7/2}, 1d_{5/2})^{\pi}$	11.732	0.156	−0.727	3.304
$(2p_{3/2}, 2s_{1/2})^{\pi}$	12.444	0.148	0.373	1.726
$(2p_{1/2}, 2s_{1/2})^{\pi}$	14.133	0.003	−0.043	−1.233
$(2p_{3/2}, 1d_{3/2})^{\pi}$	12.120	0.003	−0.015	0.451
$(2p_{1/2}, 1d_{3/2})^{\pi}$	13.809	0.073	0.166	1.053
$(1f_{5/2}, 1d_{3/2})^{\pi}$	13.867	0.018	0.250	2.756
$(2p_{3/2}, 1d_{5/2})^{\nu}$	15.683	0.000	0.012	1.410
$(2p_{3/2}, 2s_{1/2})^{\nu}$	11.773	0.015	−0.079	1.737
$(2p_{3/2}, 1d_{3/2})^{\nu}$	10.329	0.040	0.038	0.456
$(2p_{1/2}, 1d_{3/2})^{\nu}$	12.112	0.001	−0.016	1.084
$(1g_{9/2}, 1f_{7/2})^{\nu}$	11.364	0.003	−0.106	4.171
Partial Sum		0.461	−0.147	
Total Sum		0.465	−0.163	

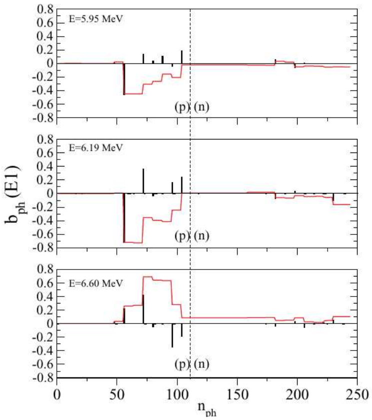

ph conf.	$E = 6.19$ MeV			F^{λ}_{ph}
	E (MeV)	A_{ph}	$b_{ph}(E1)$	
$(1f_{7/2}, 1d_{5/2})^{\pi}$	11.732	0.156	-0.727	3.304
$(2p_{3/2}, 2s_{1/2})^{\pi}$	12.444	0.148	0.373	1.726
$(2p_{1/2}, 2s_{1/2})^{\pi}$	14.133	0.003	-0.043	-1.233
$(2p_{3/2}, 1d_{3/2})^{\pi}$	12.120	0.003	-0.015	0.451
$(2p_{1/2}, 1d_{3/2})^{\pi}$	13.809	0.073	0.166	1.053
$(1f_{5/2}, 1d_{3/2})^{\pi}$	13.867	0.018	0.250	2.756
$(2p_{3/2}, 1d_{5/2})^{\nu}$	15.683	0.000	0.012	1.410
$(2p_{3/2}, 2s_{1/2})^{\nu}$	11.773	0.015	-0.079	1.737
$(2p_{3/2}, 1d_{3/2})^{\nu}$	10.329	0.040	0.038	0.456
$(2p_{1/2}, 1d_{3/2})^{\nu}$	12.112	0.001	-0.016	1.084
$(1g_{9/2}, 1f_{7/2})^{\nu}$	11.364	0.003	-0.106	4.171
Partial Sum		0.461	-0.147	
Total Sum		0.465	-0.163	

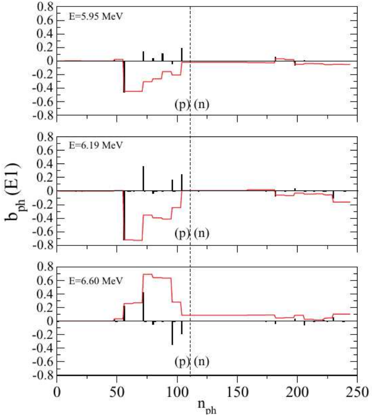

Several 1p-1h configurations participate but not coherently

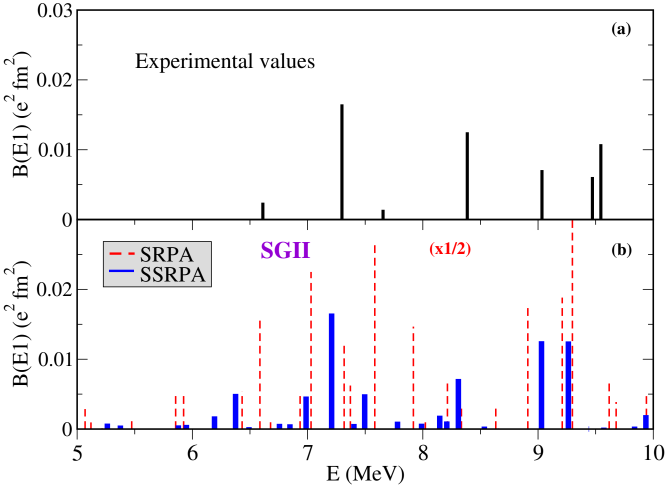

D. Gambacurta , M. Grasso , O. Vasseur, Physics Letters B 777 (2018) 163–168

	Exp	SRPA SGII	SSRPA SGII	SRPA SLy4	SSRPA SLy4
$\sum B(E1)$	0.068 $\pm$ 0.008	0.563	0.078	1.012	0.126
$\sum_i E_i B_i(E1)$	0.570 $\pm$ 0.062	4.618	0.621	8.795	1.062

Experimental and theoretical $\sum B(E1)$ in (e^2 fm^2) and $\sum_i E_i B_i(E1)$ in (MeV e^2 fm^2) summed between 5 and 10 MeV.
From D. G., M. Grasso , O. Vasseur, Physics Letters B 777 (2018) 163–168

Total $B(E1)$ and EWSRs (From 5 to 10 MeV)

	Exp	SRPA SGII	SSRPA SGII	SRPA SLy4	SSRPA SLy4
$\sum B(E1)$	0.068 $\pm$ 0.008	**0.563**	**0.078**	1.012	0.126
$\sum_i E_i B_i(E1)$	0.570 $\pm$ 0.062	**4.618**	**0.621**	8.795	1.062

Experimental and theoretical $\sum B(E1)$ in (e^2 fm^2) and $\sum_i E_i B_i(E1)$ in (MeV e^2 fm^2) summed between 5 and 10 MeV.
From D. G., M. Grasso , O. Vasseur, Physics Letters B 777 (2018) 163–168

SSRPA vs Data, GDR case

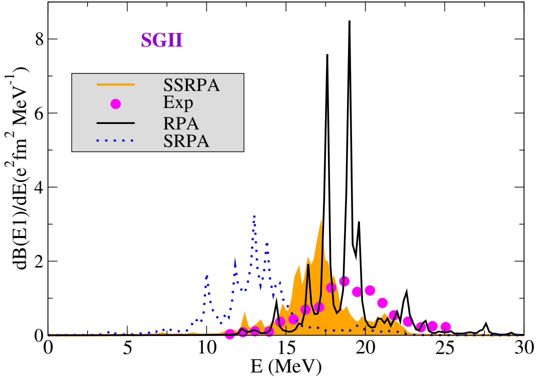

Data From J. Birkhan *et al.*, Phys. Rev. Lett. 118, 252501 (2017);
Theoretical results folded with a Lorentzian having a width of 0.25 MeV
D. G., M. Grasso , O. Vasseur, Physics Letters B 777 (2018) 163–168

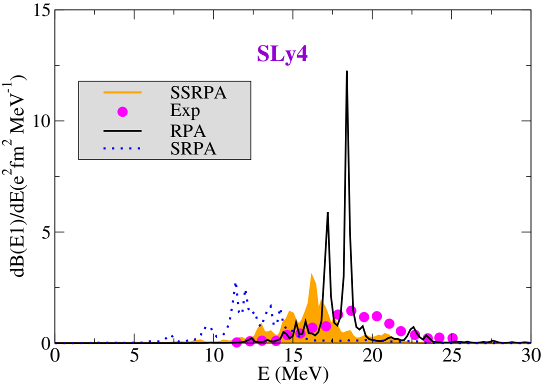

Data From J. Birkhan *et al.*, Phys. Rev. Lett. 118, 252501 (2017);
Theoretical results folded with a Lorentzian having a width of 0.25 MeV
D. G., M. Grasso , O. Vasseur, Physics Letters B 777 (2018) 163–168

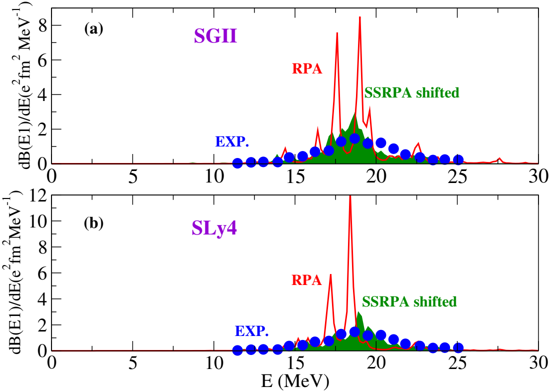

Shift $\sim$ 1 MeV (SGII), $\sim$ 2 MeV (SLy4);

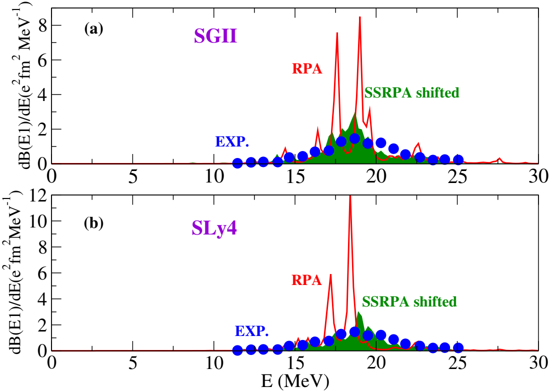

Shift $\sim$ 1 MeV (SGII), $\sim$ 2 MeV (SLy4);
Room to improve on that (overcoming the diagonal approximation in subtraction)

Dipole Polarizability

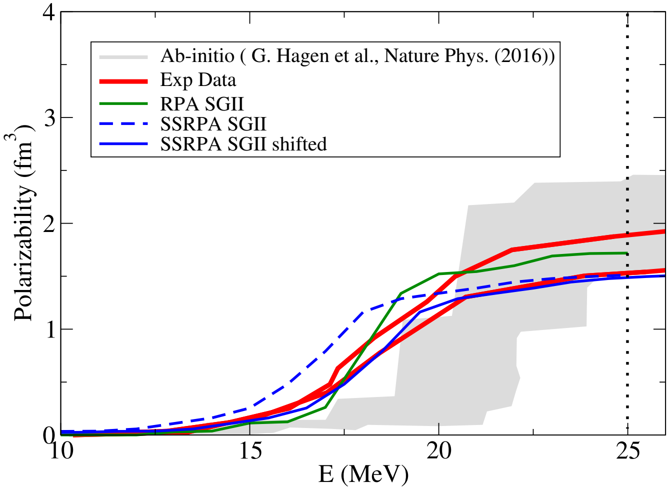

Low-energy dipole states in ^{68}Ni

- We study low–energy dipole excitations in ^{68}Ni within the SSRPA
- Strength distributions are compared with available experimental data
- Transition densities of some selected (low-lying) peaks are analyzed.
- We estimate beyond–mean–field (BMF) on the symmetry energy (J) and on its slope (L)
- M. Grasso and DG Phys. Rev. 101, 064314 (2020)

Experimental measurements: relativistic Coulomb excitations at GSI

- (I) O. Wieland et al., Phys. Rev. Lett. 102, 092502 (2009): strength centered at around 11 MeV with a contribution of 5% to the EWSR
- (II) D.M. Rossi et al., Phys. Rev. Lett. 111, 242503 (2013): strength centered at around 9.55 MeV with a contribution of 2.8% to the EWSR
- The discrepancy in the value of the centroid was explained as a possible 'energy–dependent branching ratio'.

Low-energy dipole states in ^{68}Ni

- We study low–energy dipole excitations in ^{68}Ni within the SSRPA
- Strength distributions are compared with available experimental data
- Transition densities of some selected (low-lying) peaks are analyzed.
- We estimate beyond–mean–field (BMF) on the symmetry energy (J) and on its slope (L)
- M. Grasso and DG Phys. Rev. 101, 064314 (2020)

Experimental measurements: relativistic Coulomb excitations at GSI

- (I) O. Wieland et al., Phys. Rev. Lett. 102, 092502 (2009): strength centered at around 11 MeV with a contribution of 5% to the EWSR
- (II) D.M. Rossi et al., Phys. Rev. Lett. 111, 242503 (2013): strength centered at around 9.55 MeV with a contribution of 2.8% to the EWSR
- The discrepancy in the value of the centroid was explained as a possible 'energy–dependent branching ratio'.
- Isoscalar excitation on ^{12}C target @ LNS: peak located around 10 MeV with a contribution of 10% to the EWSR (N.S. Martorana et al., Phys. Lett. B 782, 112 (2018))

Low-energy dipole states in ^{68}Ni

- We study low–energy dipole excitations in ^{68}Ni within the SSRPA
- Strength distributions are compared with available experimental data
- Transition densities of some selected (low-lying) peaks are analyzed.
- **We estimate beyond–mean–field (BMF) on the symmetry energy (J) and on its slope (L)**
- M. Grasso and DG Phys. Rev. 101, 064314 (2020)

Employed linear correlations

- Percentage of EWSR and L:
  A. Klimkiewicz et al., Phys. Rev. C 76, 051603 (R) (2007); A. Carbone et al., Phys. Rev. C 81, 041301 (R) (2010)
- L and neutron–skin thickness:
  M. Centelles et al., Phys. Rev. Lett. 102, 122502 (2009); M. Wardaet al.,, Phys. Rev. C 80, 024316 (2009)
- Neutron–skin thickness and electric dipole polarizability times the J coefficient: X. Roca-Maza et al. Phys. Rev. C 92, 064304 (2015).

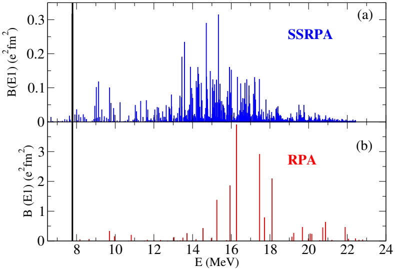

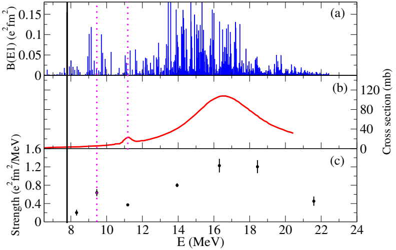

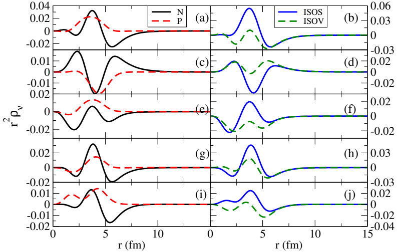

Peaks located at 9.14 ((a) and (b)), 9.70 ((c) and (d)), 10.25 ((e) and (f)), 11.10 ((g) and (h)), and 11.31 ((i) and (j))

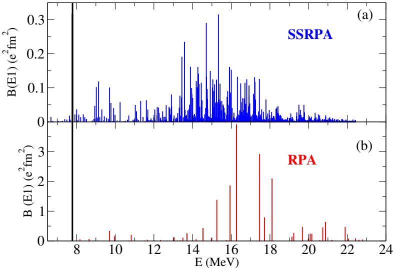

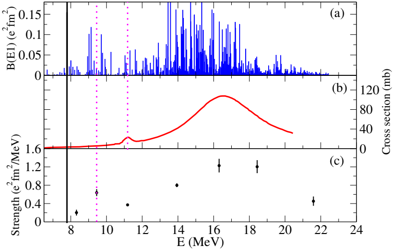

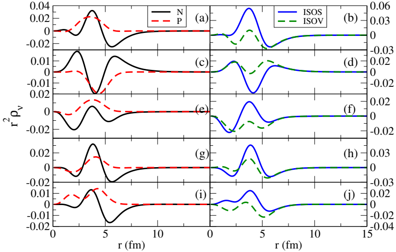

Peaks located at 9.14 ((a) and (b)), 9.70 ((c) and (d)), 10.25 ((e) and (f)), 11.10 ((g) and (h)), and 11.31 ((i) and (j))

Skyrme	J (MeV)	L (MeV)
SIII	28.16	9.90
SGII	26.83	37.70
SkI4	29.50	60.00
SkI3	34.27	100.49

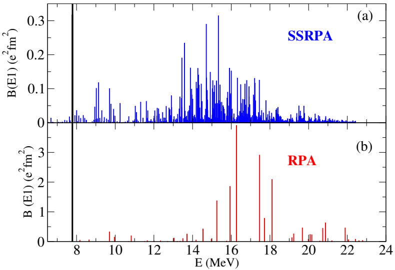

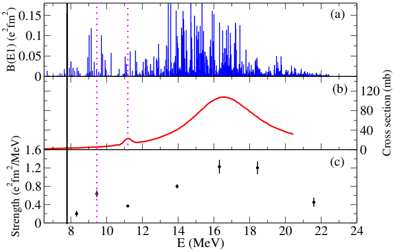

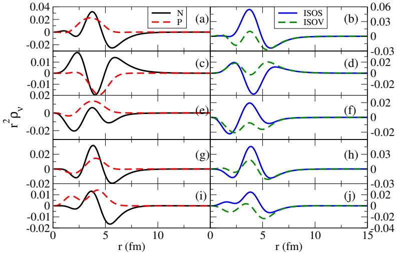

Peaks located at 9.14 ((a) and (b)), 9.70 ((c) and (d)), 10.25 ((e) and (f)), 11.10 ((g) and (h)), and 11.31 ((i) and (j))

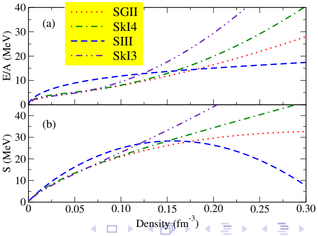

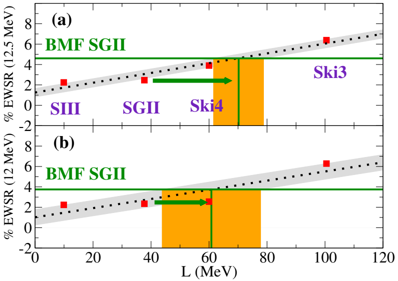
(a)
BMF SGII
Ski3
SIII
SGII
Ski4
(b)
BMF SGII
% EWSR (12.5 MeV)
% EWSR (12 MeV)
L (MeV)
-2
0
2
4
6
8
0
20
40
60
80
100
120

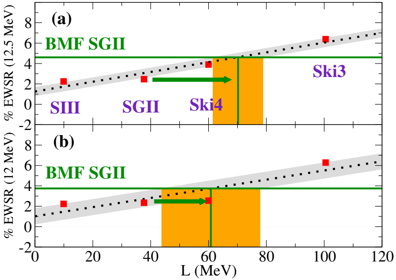

SGII(RPA)= 2.35 %
SGII(SSRPA)=3.75 %

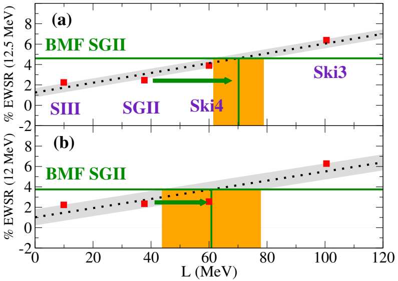

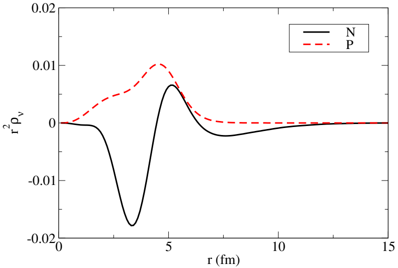

SGII(RPA)= 2.35 %
SGII(SSRPA)=3.75 %

Neutron and proton transition densities for the state located at 12.17 MeV.

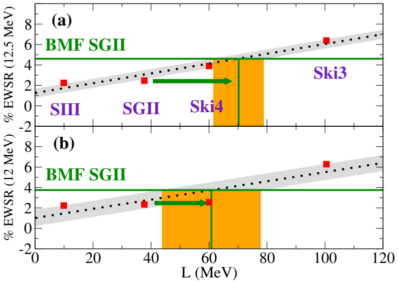
(a)
BMF SGII
Ski3
SIII
SGII
Ski4
(b)
BMF SGII
% EWSR (12.5 MeV)
% EWSR (12 MeV)
L (MeV)

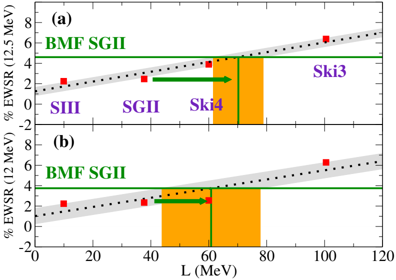
(a)
BMF SGII
Ski3
SIII
SGII
Ski4
% EWSR (12.5 MeV)
(b)
BMF SGII
% EWSR (12 MeV)
L (MeV)

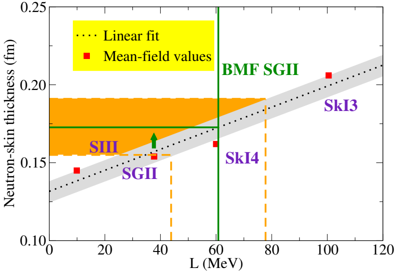
Linear fit
Mean-field values
BMF SGII
SkI3
SIII
SGII
SkI4
Neutron-skin thickness (fm)
L (MeV)

Beyond-mean-field effects on the symmetry energy and its slope

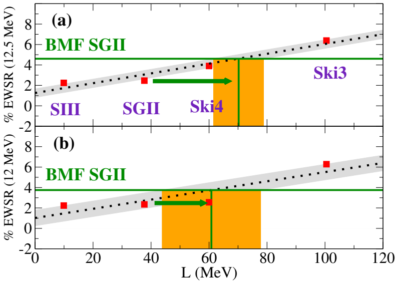

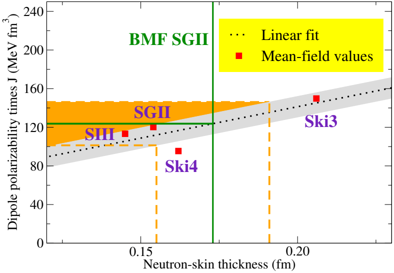

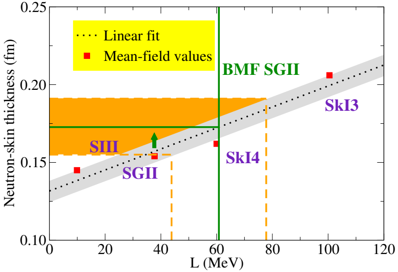

Beyond-mean-field effects on the symmetry energy and its slope

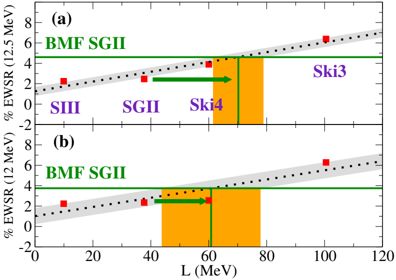

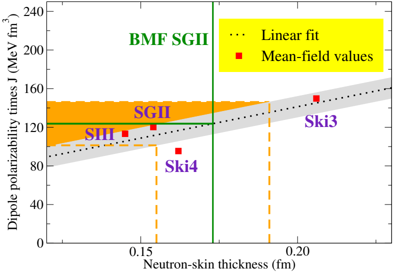

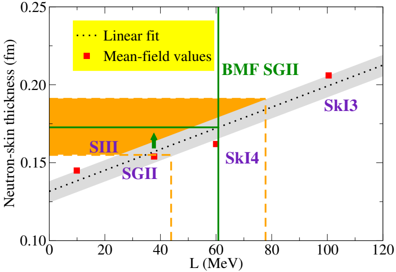

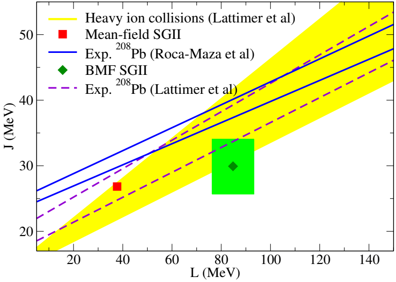

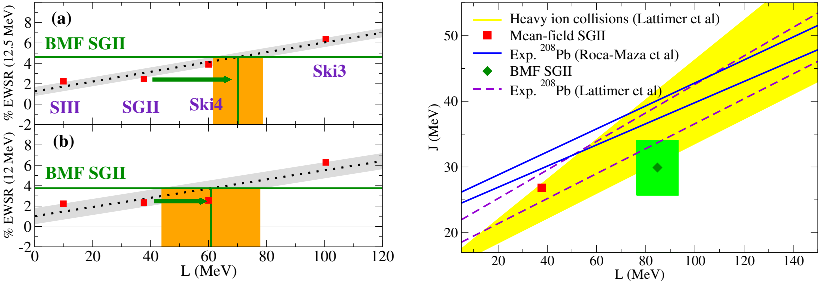

	L (MeV)	Δr_{np} (fm)	J (MeV)
Mean field	37.70	0.154	26.83
BMF	60.815 $\pm$ 16.982	0.173 $\pm$ 0.018	27.617 $\pm$ 5.004

Monopole response in RPA and SSRPA

- Evolution of the response in Ca isotopes from ^{40}Ca to ^{60}Ca [a]
- $N = 20$ isotones : ^{40}Ca, ^{36}S and ^{34}Si
- The case of ^{68}Ni

[a] Phys. Rev. Lett. 121, (2018) @ RIKEN

The key-points of our study

- Soft monopole modes driven by neutron excitations
- Not only at the surface of the nucleus but over its entire volume
- Properties are discussed as a function of the isospin asymmetry
- More details: DG, M. Grasso and O. Sorlin, PRC 100, 014317 (2019)

Monopole strength distribution in Ca isotopes

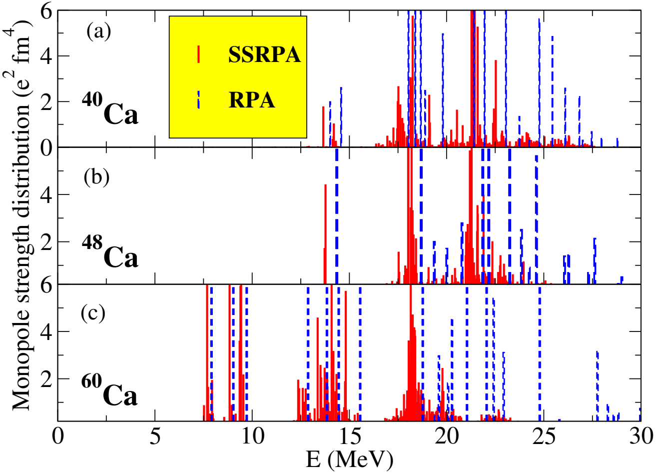

(a) Monopole strength distribution computed with RPA (dashed blue bars) and SSRPA (full red bars) for ^{40}Ca; (b) Same as in (a) but for ^{48}Ca; (c) Same as in (a) but for ^{60}Ca.

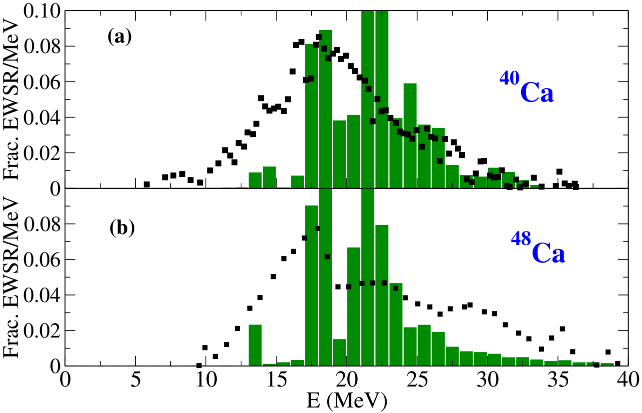

(a) Black squares: experimental results ; green bars: SSRPA predictions for ^{40}Ca; (b) Same as in (a) but for ^{48}Ca.

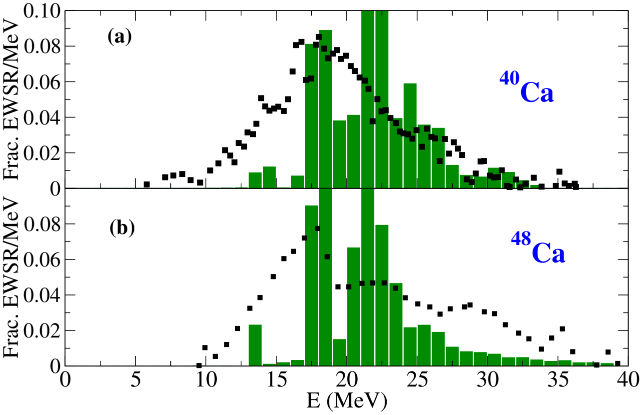

(a) Black squares: experimental results ; green bars: SSRPA predictions for ^{40}Ca; (b) Same as in (a) but for ^{48}Ca.

Centroids (MeV)

^{40}Ca: 21.3 (RPA), 20.7 (SSRPA), 18.3 (Exp)

^{48}Ca: 20.7 (RPA), 20.4 (SSRPA), 19.0 (Exp)

Transition densities in ^{40}Ca

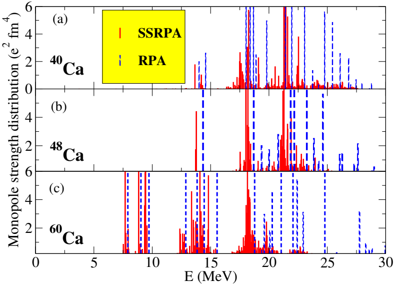

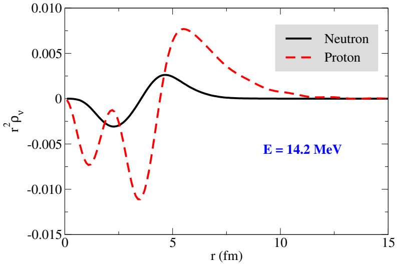

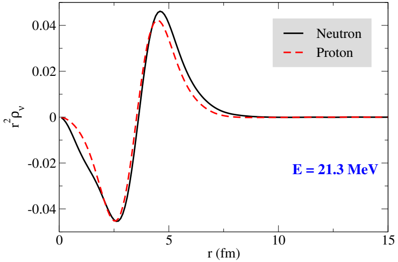

Transition densities in ^{48}Ca

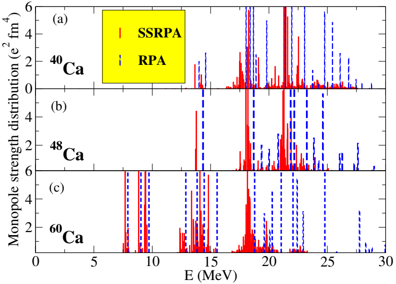

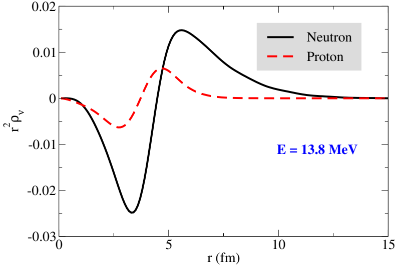

Transition densities in ^{60}Ca

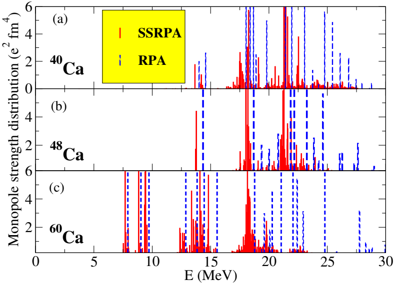

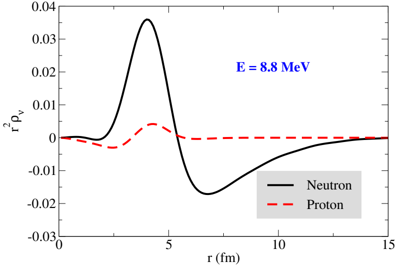

Transition densities in ^{60}Ca

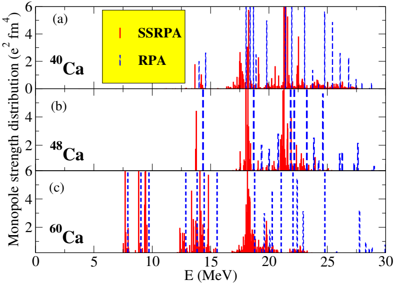

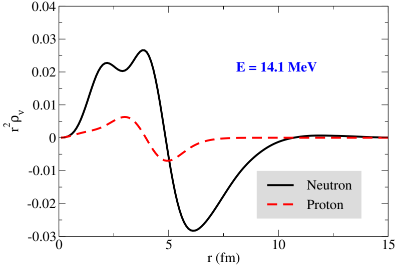

Monopole strength distribution in ^{34}Si and ^{36}S

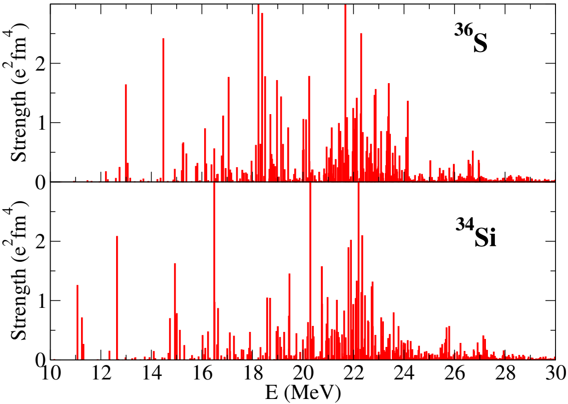

Monopole isoscalar strength distributions calculated for the nuclei ^{36}S (a) and ^{34}Si (b).

Transition densities in ^{34}Si and ^{36}S

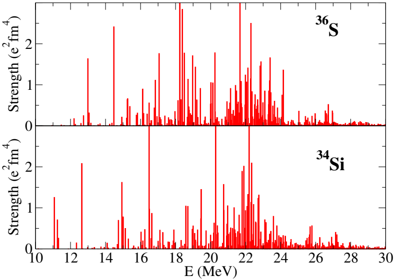

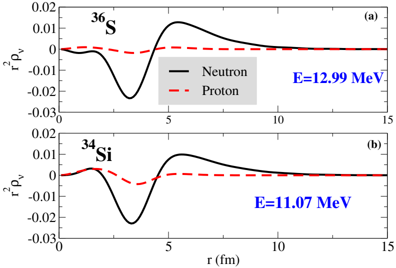

Composition of the peak located at 11.07 (12.99) MeV for ^{34}Si (^{36}S).

^{34}Si	1p1h 54 %	2p2h 46 %
	$[\nu 2d_{3/2}, \nu 1d_{3/2}]^{J=0}$	$[[\pi 3p_{1/2}, \nu 3f_{7/2}]^{J_p=3}[\pi 1d_{5/2}, \nu 2s_{1/2}]^{J_h=3}]^{J=0}$
		$[[\pi 4p_{1/2}, \nu 1f_{5/2}]^{J_p=2}[\pi 1d_{5/2}, \nu 2s_{1/2}]^{J_h=2}]^{J=0}$
		$[[\pi 4p_{1/2}, \nu 1f_{5/2}]^{J_p=3}[\pi 1d_{5/2}, \nu 2s_{1/2}]^{J_h=3}]^{J=0}$
		$[[\pi 6s_{1/2}, \nu 2d_{3/2}]^{J_p=2}[\pi 1d_{5/2}, \nu 1d_{3/2}]^{J_h=2}]^{J=0}$
		$[[\pi 6s_{1/2}, \nu 2d_{5/2}]^{J_p=2}[\pi 1d_{5/2}, \nu 1d_{3/2}]^{J_h=2}]^{J=0}$
		$[[\pi 3d_{3/2}, \nu 3s_{1/2}]^{J_p=2}[\pi 1d_{5/2}, \nu 1d_{3/2}]^{J_h=2}]^{J=0}$
		$[[\pi 3d_{3/2}, \nu 2d_{5/2}]^{J_p=1}[\pi 1d_{5/2}, \nu 1d_{3/2}]^{J_h=1}]^{J=0}$
		$[[\pi 3d_{3/2}, \nu 2d_{5/2}]^{J_p=2}[\pi 1d_{5/2}, \nu 1d_{3/2}]^{J_h=2}]^{J=0}$
^{36}S	1p1h 52 %	2p2h 48 %
	$[\nu 2d_{3/2}, \nu 1d_{3/2}]^{J=0}$	$[[\pi 3d_{3/2}, \nu 4d_{3/2}]^{J_p=2}[\pi 1d_{5/2}, \nu 1d_{3/2}]^{J_h=2}]^{J=0}$
		$[[\pi 4d_{3/2}, \nu 4s_{1/2}]^{J_p=2}[\pi 2s_{1/2}, \nu 1d_{3/2}]^{J_h=2}]^{J=0}$
		$[[\pi 4d_{3/2}, \nu 5s_{1/2}]^{J_p=1}[\pi 2s_{1/2}, \nu 1d_{3/2}]^{J_h=1}]^{J=0}$
		$[[\pi 4d_{3/2}, \nu 4d_{3/2}]^{J_p=2}[\pi 2s_{1/2}, \nu 1d_{3/2}]^{J_h=2}]^{J=0}$
		$[[\pi 4d_{3/2}, \nu 2d_{5/2}]^{J_p=1}[\pi 2s_{1/2}, \nu 1d_{3/2}]^{J_h=1}]^{J=0}$

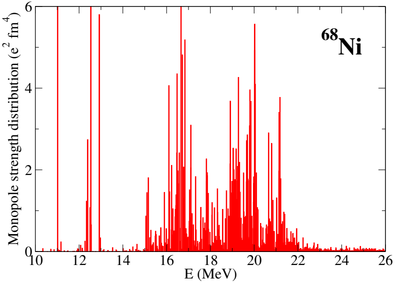
68Ni
Monopole strength distribution (e^2 fm^4)
E (MeV)
0
2
4
6
10
12
14
16
18
20
22
24
26

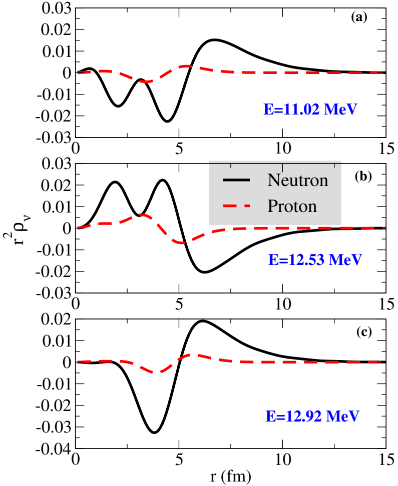
(a)
E=11.02 MeV
(b)
Neutron
Proton
E=12.53 MeV
(c)
E=12.92 MeV
$r^2\rho_\nu$
r (fm)

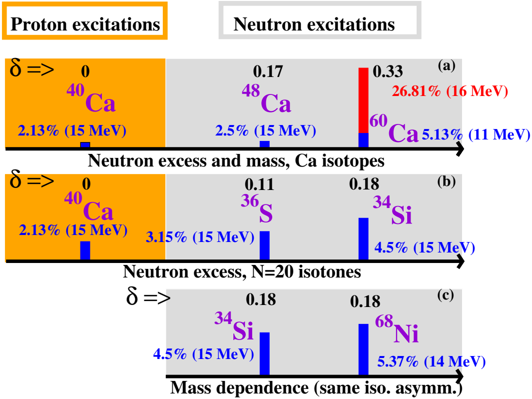

Percentages of the EWSR for several nuclei and corresponding isospin asymmetry $\delta = (N - Z)/A$.
(a) Ca isotopes: evolution as a function of the neutron excess and the mass;
(b) $N = 20$ isotones: evolution as a function of the neutron excess;
(c) Evolution as a function of the mass for two nuclei with the same isospin asymmetry, ^{34}Si and ^{68}Ni.

Recent extension to the charge exchange (CE) case

Second RPA for CE excitations

- Extension of the Subtracted SRPA (SSRPA) to the treatment of **CE excitations**
- First applications to ^{48}Ca (lightest double-β emitter) and ^{78}Ni in Ref [1]
- More applications (^{14}C, ^{22}O, ^{90}Zr and ^{132}Sn) in Ref [2]

More details in:

[1] D.Gambacurta, M. Grasso, J. Engel, Phys. Rev. Lett. 125, 212501 (2020)
[2] D.Gambacurta and M. Grasso, Phys. Rev. C 105, 014321, (2022)

The quenching problem

- Computed GT matrix elements **are larger** than the experimental ones.
- The problem is "cured" by **quenching** the strength by $q \sim 0.7$ or using effective axial constant g_A (~ 1) instead of the "bare" value ~ 1.27.

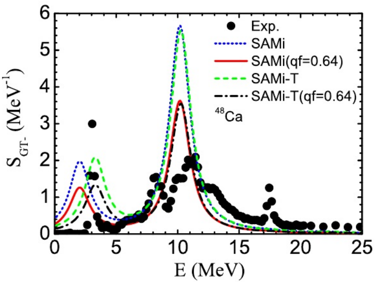

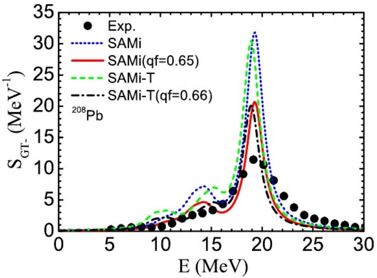

$$qf = \frac{\sum_{E_x=0}^{E_x(\max)} B(GT : E_x)_{\text{expt}}}{\sum_{E_x=0}^{E_x(\max)} B(GT)_{\text{calc}}}$$

Li-Gang Cao , Shi-Sheng Zhang, and H. Sagawa, PHYSICAL REVIEW C **100**, 054324 (2019)

Skyrme-RPA calculations

GT$^-$ Strength Distribution ^{48}Ca, SGII interaction

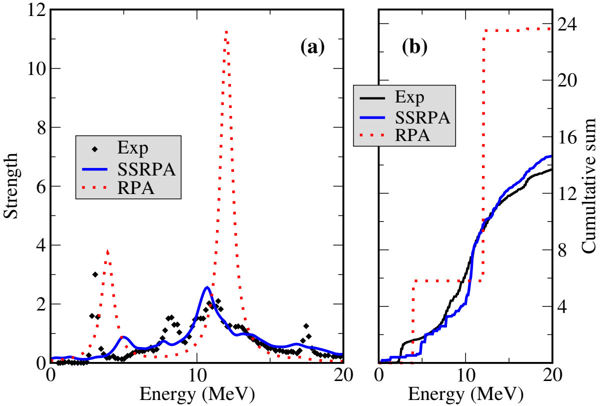

(a) GT$^-$ strength in RPA and SSRPA compared with (GT$^-$ plus IVSM) data.
(b) Cumulative strengths up to 20 MeV.
Data from: K. Yako *et al.*, Phys. Rev. Lett. 103, 012503 (2009)

From D.Gambacurta, M. Grasso, J. Engel, Phys. Rev. Lett. 125, 212501 (2020)

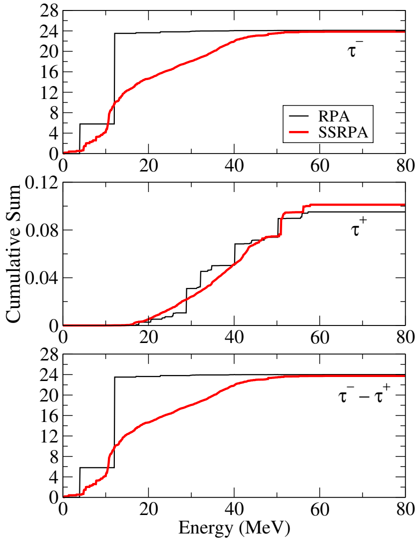
RPA
SSRPA
τ⁻
τ⁺
τ⁻ − τ⁺
Cumulative Sum
Energy (MeV)

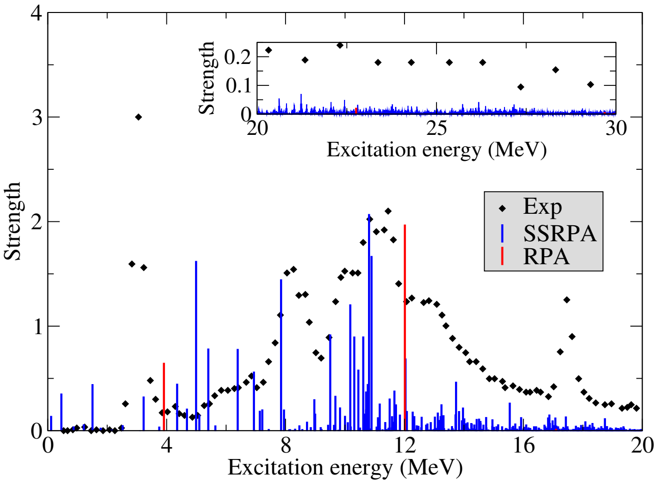

Experimental GT$^-$ in MeV^{-1} and discrete RPA and SSRPA strength distributions (no units) obtained with the Skyrme parameterization SGII, for ^{48}Ca . The RPA strength has been divided by nine and the SSRPA strength by two.

From D.Gambacurta, M. Grasso, J. Engel, Phys. Rev. Lett. 125, 212501 (2020)

GT$^-$ Strength Distribution ^{48}Ca

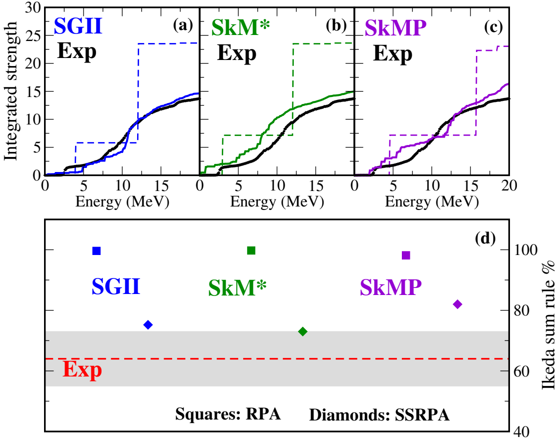

(a), (b), (c) Strengths integrated up to 20 MeV with different parameterizations.

(d) RPA and SSRPA percentages of the Ikeda sum rule below 30 MeV compared with the experimental one.

From D.Gambacurta, M. Grasso, J. Engel, Phys. Rev. Lett. 125, 212501 (2020)

GT$^-$ Strength Distribution and β-decay half-life ^{78}Ni

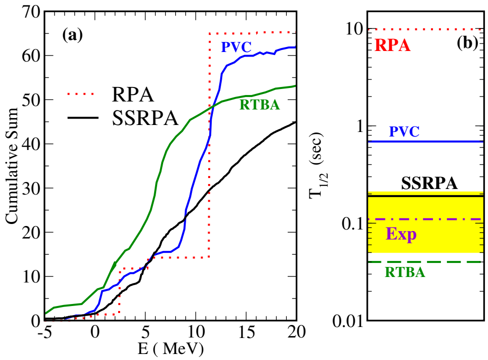

(a) Cumulative sum for the nucleus ^{78}Ni within the SSRPA, PVC and RTBA models;
(b) β-decay half-life for ^{78}Ni. **No quenching, bare $g_a = 1.27$;**
Data from: P. T. Hosmer *et al.* Phys. Rev. Lett. 94, 112501 (2005)
PVC: Y. F. Niu, G. Coló and E. Vigezzi, Phys. Rev. C 90, 054328 (2014)
RTBA:C. Robin and E. Litvinova, Phys. Rev. C 98, 051301(R), 2018

From D.Gambacurta, M. Grasso, J. Engel, Phys. Rev. Lett. 125, 212501 (2020)

GT$^-$ Strength Distribution ^{90}Zr and ^{132}Sn, interaction dependence

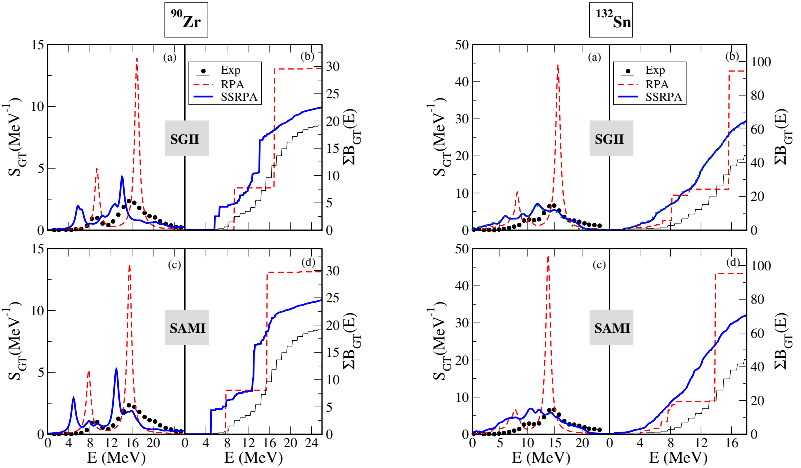

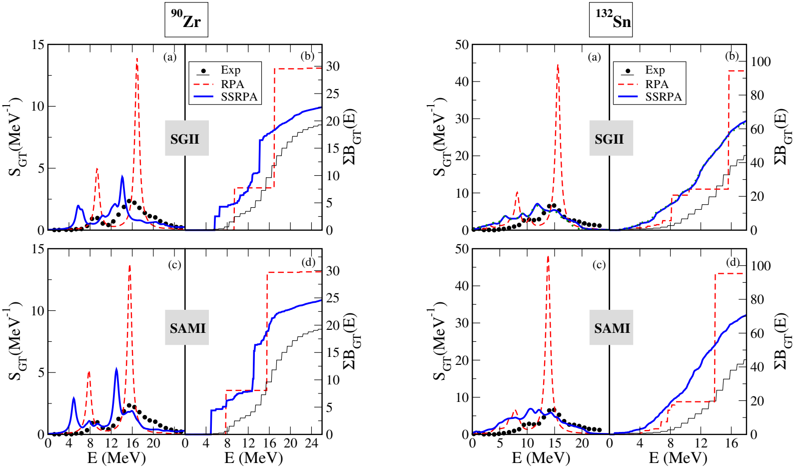

Other sources of queenching may be needed ...

Conclusions

- The SSRPA provides a richer and more general description of nuclear excitations (2p-2h configurations $\Rightarrow$ fragmentation and width)
- Better agreement data
- Dipole response in ^{48}Ca and ^{68}Ni
- BMF effects on the symmetry energy (J) and its slope (L): qualitative estimation (BMF effects increase both J and L)
- Soft monopole excitations: "neutron-driven" excitations in neutron–rich systems, extending in the entire volume, 1p-1h nature
- GT strength and β-decay half-life, considerable improvement with respect to the RPA $\Rightarrow$ Single and Double Charge Exchange excitations, Neutrinoless Double Beta Decay

Thanks For Your Attention !!!